Evolution, 2025, **79**(**12**), 2597–2611
https://doi.org/10.1093/evolut/qpaf191
Advance access publication 26 September 2025
Methods Article

Quantifying feedback among traits in coevolutionary models

Xiaoyan Long [1], **Jussi Lehtonen** [2], **Jonathan M. Henshaw** [1]

[1]Institute of Biology I, University of Freiburg, Freiburg im Breisgau, Germany
[2]Department of Biological and Environmental Science, University of Jyvaskyla, Jyväskylä, Finland

Corresponding author: Institute of Biology I, University of Freiburg, Hauptstraße 1, D-79104 Freiburg, Germany. Email: xiaoyan.long2@gmail.com

Abstract

Phenotypic traits rarely evolve in isolation. Instead, multiple traits typically interact to influence fitness, resulting in complex coevolutionary dynamics. Such dynamics can be predicted using mathematical frameworks, such as adaptive dynamics and quantitative genetics. Selection gradients play a crucial role in these frameworks, describing the direction and strength of selection and thus predicting evolutionary trajectories and potential endpoints. Current theory focuses mainly on analysing how traits change in response to selection, which changes over time as traits evolve. However, the extent to which changes in each trait contribute to changes in the selection environment remains unquantified, leaving much of our understanding of trait coevolution reliant on verbal reasoning. To advance a more comprehensive and quantitative understanding of coevolutionary dynamics, we develop a general framework that examines how trait changes feedback to influence the selection environment. This framework enables a fine-grained and systematic investigation of coevolutionary feedback between traits and selection gradients by quantifying the pathways through which they influence one another. Our framework can be applied both to adaptive-dynamic models and to quantitative-genetic models under the weak selection limit. We illustrate our approach with three examples that showcase its potential to deepen our understanding of established models.

Keywords: joint evolution, adaptive dynamics, quantitative genetics, selection gradient, canonical equation, anisogamy

Introduction

In nature, it is rare for one trait to evolve independently of the rest of an organism's phenotype. Instead, multiple traits typically interact to determine an organism's fitness, resulting in often complex coevolutionary dynamics (Bank, 2022; Svensson et al., 2021). Here are three examples of this ubiquitous phenomenon, taken from our own field of behavioral ecology: First, sex role divergence often involves the coevolution of male and female traits, including parental care, mate choice, and mating competition (Andersson, 1994; Fromhage & Jennions, 2016; Henshaw et al., 2019; Long & Weissing, 2023). Second, natal dispersal is suggested to coevolve with prosocial behaviours (e.g., helping other members in a group; see Hochberg et al., 2008; McNamara & Leimar, 2020; Mullon et al., 2018; Powers et al., 2011). Third, in group-foraging species foraging strategies coevolve with vigilance against predators (Giraldeau & Caraco, 2000; Harten et al., 2018; Mathot & Giraldeau, 2008; Ranta et al., 1998).

Our understanding of coevolutionary dynamics depends critically on theoretical models based on a range of approaches, including population genetics (Kirkpatrick, 1982; Nagylaki, 1992; Revathi Venkateswaran et al., 2021), quantitative genetics (Lande, 1981; Mead & Arnold, 2004; Roff, 1997), adaptive dynamics (Dashtbali et al., 2024; Fawcett et al., 2011; Henshaw et al., 2019), and individual-based simulations (Baldauf et al., 2014; Long & Weissing, 2023; Waffender & Henshaw, 2023; Long et al., 2025a). Here, our primary focus is on the adaptive-dynamic framework. By separating the processes of mutation, selection, and demographic or ecological change, adaptive dynamics enables us to focus on phenotypic, rather than genetic, evolution. This facilitates models of complex trait interactions, including frequency-dependent selection and demographic structure (Kuijper et al., 2012; Pen & Weissing, 2001). In adaptive-dynamic models, rare mutations of small effect are assumed to arise against the background of a monomorphic resident population (where all other individuals share the same phenotype). The relationship between mutational effects and mutant fitness is quantified as a selection gradient, which describes the direction and strength of selection acting on a trait. Selection gradients can then be used to predict evolutionary trajectories and the likely end points of evolution (e.g., evolutionarily stable strategies, see Dercole & Rinaldi, 2008; Geritz et al., 1998; McGill & Brown, 2007).

Selection gradients are a key determinant of evolutionary change in adaptive dynamics and many other modeling frameworks (e.g., Lande & Arnold, 1983; Taylor, 1996). Crucially, selection gradients themselves also change over evolutionary time, for two reasons. First, selection is often frequency-dependent, so that the relationship between trait values and fitness (i.e., the fitness function) changes along with the population trait distribution. Second, since selection gradients depend on the statistical relationship between trait values and fitness within a population, they depend on the current trait distribution even when the fitness function is held fixed. Selection's dependence on the trait distribution

Received May 9, 2025; revisions received September 3, 2025; accepted September 14, 2025
Associate Editor: Vincent Calcagno; Handling Editor: Jason Wolf

in turn has important implications for coevolution, because it induces a feedback loop: Selection causes traits to change, leading to changes in the current trait distribution, which can subsequently alter the strength and direction of selection. Further, just as selection on one trait can indirectly cause changes in other traits due to genetic correlations (Lande & Arnold, 1983), changes in the distribution of one trait can affect selection on other coevolving traits, because fitness is often determined by an interaction between traits (Bank, 2022; Svensson et al., 2021). Our current mathematical toolkit mainly focuses on analysing one half of this feedback loop: the effects of selection on trait evolution. While some studies have applied basic causal analysis, such as switching off evolutionary change in one trait to observe how this affects selection on another (e.g., Maisonneuve & Aubier, 2025), these approaches do not precisely quantify how much each trait's change contributes to changes in the selection environment for itself and for other traits. As a result, a quantitative decomposition is lacking, and thus, our understanding of trait coevolution continues to rely largely on verbal reasoning about causal relationships over evolutionary time.

Here, we develop a general framework for analysing feedback between traits and selection gradients in coevolutionary models. Our goal is to enhance our understanding of trait coevolution by providing a formal tool to examine how traits interact to shift the selection environment. Instead of relying solely on verbal explanations of coevolutionary dynamics, our approach offers a means of quantifying feedbacks. Our framework can be applied to adaptive-dynamic models and also to quantitative genetic models under the assumption of weak selection. We illustrate these applications via three examples, revealing our framework's potential to enrich our understanding of even well-established models.

General approach

Adaptive dynamics for a single trait

We begin by outlining the fundamental assumptions of adaptive-dynamic models of evolutionary change, as encapsulated by the "canonical equation" (Champagnat et al., 2001; Dieckmann & Law, 1996). In adaptive dynamics, the resident population is assumed to be genetically monomorphic at any given point in time. Mutations arise rarely and cause only small deviations from the resident phenotype, corresponding to small differences in fitness (i.e., adaptive dynamics is inherently a weak selection framework). If a mutant trait value outperforms the resident strategy in fitness terms, there is a nonzero probability that it invades the resident population, and eventually completely replaces the resident strategy. Since mutations are rare, it is assumed that each invasion is completed before a new mutation arises. This process typically continues until the population reaches an equilibrium state, at which point no further mutant invasions are possible. The dynamics of this process are captured by the canonical equation of adaptive dynamics (Dieckmann & Law, 1996). In a one-trait model with a resident trait z, the canonical equation takes the form:

$$\frac{dz}{dt} = \frac{1}{2}\mu N \sigma_{zz} \beta_z, \tag{1}$$

where μ is the mutation rate of the trait at birth; N is the size of the resident population; σ_{zz} is the variance in the phenotypic effects of mutations (given by $\sigma_{zz} = \mathbb{E}(\hat{z} - z)^2$, where $\hat{z}$ is the trait value of a mutant); the selection gradient $\beta_z = \frac{1}{\bar{w}} \frac{\partial}{\partial \hat{z}} w(\hat{z}, \ z)|_{\hat{z}=z}$ describes the strength and direction of selection on the trait z (where $w(\hat{z}, \ z)$ denotes the fitness of a mutant with trait $\hat{z}$ in a monomorphic resident population with trait z, and $\bar{w}$ indicates the mean fitness of resident individuals); and the factor $\frac{1}{2}$ reflects that, under directional selection, only half of the mutations are beneficial and thus can contribute to evolutionary change. The factor $\kappa = \frac{1}{2}\mu N$ indicates the total number of mutations that can contribute to evolutionary change per time unit. Thus, the one-trait canonical equation can also be written as follows:

$$\frac{dz}{dt} = \kappa \sigma_{zz} \beta_z. \tag{1*}$$

Figure 1. Feedback loop between a single trait z and its selection gradient β_z in an adaptive-dynamic model. The black solid arrow indicates changes in the trait value due to selection, whereas the black dashed arrow represents changes in the selection gradient due to changing trait values.

Feedback analysis with one evolving trait

We will principally be interested in feedback acting on two or more coevolving traits. However, we will first introduce some of the necessary concepts in the setting of a single evolving trait, where things are much simpler. As shown in Figure 1, the selection gradient β_z determines the direction and scales the speed of evolutionary changes on the trait z (black solid arrow) and, reciprocally, changes in the trait value can feed back to influence the selection gradient (black dashed arrow). Using the chain rule of calculus, we can break down the rate of change in the selection gradient as follows:

$$\frac{d\beta_z}{dt} = \frac{d\beta_z}{dz}\frac{dz}{dt}. \tag{2}$$

Plugging equation (1*) into (2) then yields:

$$\frac{d\beta_z}{dt} = \kappa \sigma_{zz} \beta_z \frac{d\beta_z}{dz}. \tag{3}$$

Equation (3) describes the feedback loop acting on the selection gradient (Figure 1) in quantitative terms. To see qualitatively how such feedback affects selection, we need to examine the combination of the selection gradient β_z and its feedback term $\frac{d\beta_z}{dt}$ (Figure 2). A positive selection gradient indicates selection for trait values that are larger than the current resident strategy. When feedback is also posi-

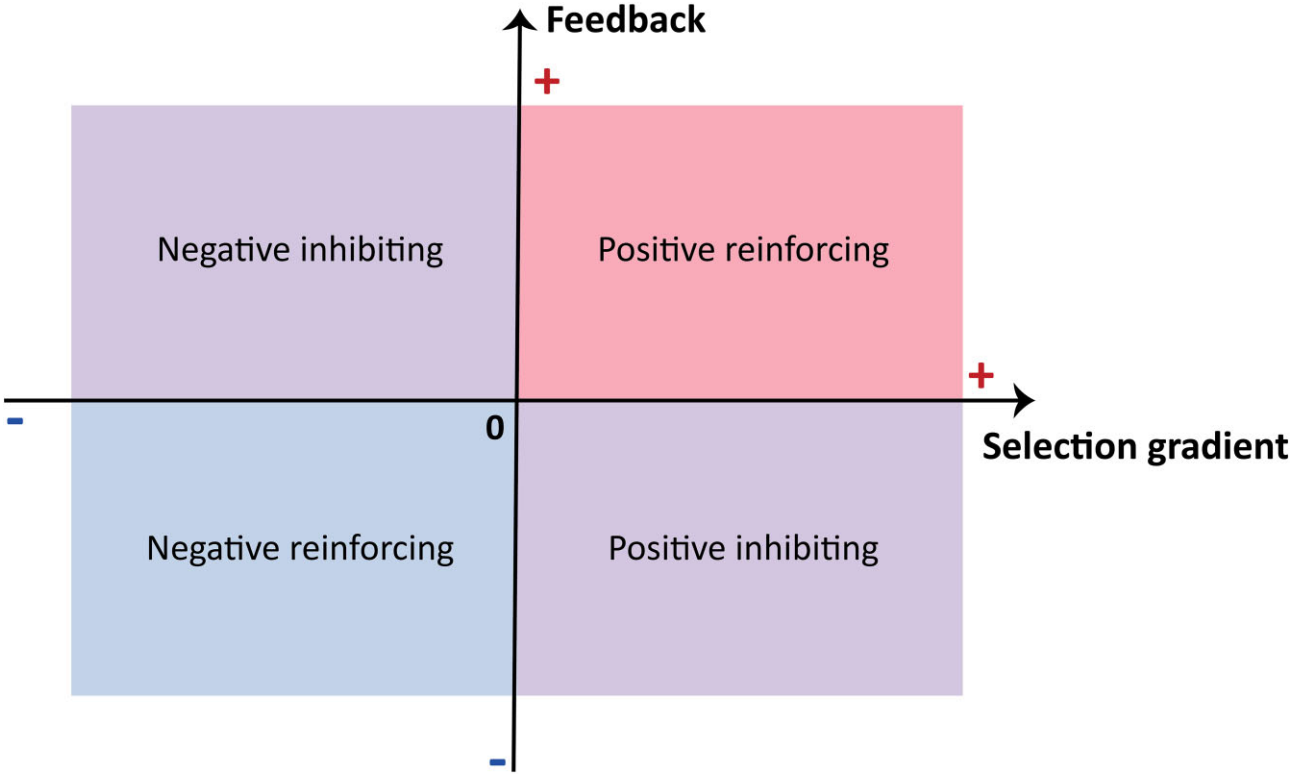

Figure 2. How does feedback influence the strength of selection on a trait? In this coordinate plot, the *x*-axis represents the selection gradient, while the *y*-axis represents the feedback (or feedback components) acting on the selection gradient (e.g., equation (3)). When both the selection gradient and feedback are positive (top-right quadrant), selection favors mutants with trait values larger than the current resident value, and feedback acts to increase the intensity of this selection (positive reinforcing selection). When the selection gradient is positive but feedback is negative (bottom-right quadrant), selection again favors larger trait values, but feedback reduces the strength of this selection (positive inhibiting selection). In the bottom-left quadrant, where both the selection gradient and feedback are negative, selection favors smaller trait values and feedback increases the strength of selection (negative reinforcing selection). Finally, in the top-left quadrant, when the selection gradient is negative but feedback is positive, selection again favors smaller trait values, but feedback acts to weaken selection (negative inhibiting selection).

tive, it intensifies this selection, making selection for a larger trait even stronger. We refer to this as "positive reinforcing" feedback. On the other hand, if the selection gradient is positive, but feedback is negative, it weakens selection for larger trait values, which we term "positive inhibiting" feedback. Analogous considerations apply when the selection gradient is negative: Negative feedback on a negative selection gradient reinforces selection ("negative reinforcing" feedback), whereas positive feedback inhibits it ("negative inhibiting" feedback). Thus, feedback can either amplify or dampen selection on a trait, depending on whether it aligns with or opposes the direction of selection gradient (see examples below).

Adaptive dynamics of two coevolving traits

When multiple traits coevolve in a single species, the evolutionary dynamics become more complicated, because traits can interact with one another. Here, we start with a model with two traits, x and y. In this case, the canonical equation takes the form:

$$\frac{dx}{dt} = \kappa\sigma_{xx}\beta_x + \kappa\sigma_{xy}\beta_y \tag{4a}$$

$$\frac{dy}{dt} = \kappa\sigma_{yy}\beta_y + \kappa\sigma_{xy}\beta_x, \tag{4b}$$

which can be written more compactly as follows:

$$\frac{d}{dt}\begin{bmatrix}x\\y\end{bmatrix} = \kappa\mathbf{M}\begin{bmatrix}\beta_x\\\beta_y\end{bmatrix}. \tag{4*}$$

Here, $\mathbf{M} = \begin{bmatrix}\sigma_{xx} & \sigma_{xy}\\ \sigma_{xy} & \sigma_{yy}\end{bmatrix}$ is the variance–covariance matrix of the phenotypic effects of new mutations, and $\kappa = \frac{1}{2}\mu N$ is defined as above. Importantly, σ_{xy} represents the mutational covariance between the two traits (i.e., the covariance between the effects of a random mutation on x and y). Such mutational covariance can affect the direction of evolution. If $\sigma_{xy} \neq 0$, then selection acts on x both directly (quantified by β_x) and indirectly via selection on y (β_y) and the mutational correlation between the two traits (σ_{xy}).

Feedback analysis with two coevolving traits

For ease of understanding, we start with the assumption that there is no mutational correlation between the coevolving traits (i.e., the off-diagonal elements of the matrix $\mathbf{M}$ equal zero), meaning that each trait is only under direct selection. This assumption is widely made in applications of adaptive dynamics. Equations (4a and 4b) then simplifies to:

$$\frac{dx}{dt} = \kappa\sigma_{xx}\beta_x \tag{5a}$$

$$\frac{dy}{dt} = \kappa\sigma_{yy}\beta_y. \tag{5b}$$

We now develop tools for studying coevolutionary feedback between two coevolving traits. In the absence of mutational correlation, such feedback arises via the following two-step process (Figure 3A): (1) Traits change due to direct selection (black solid arrows in Figure 3A). (2) The selection environment (i.e., the strength and direction of selection) changes due to the shifts in trait values (black dashed arrows in Figure 3A). In the two-trait model, each selection gradient, β_x and β_y, can be understood as a function of the current resident trait values, x and y. Similar to equation (2), we can break down changes in the selection gradients using the chain rule, as follows:

$$\frac{d}{dt}\beta_x = \frac{\partial \beta_x}{\partial x}\frac{dx}{dt} + \frac{\partial \beta_x}{\partial y}\frac{dy}{dt} \tag{6a}$$

$$\frac{d}{dt}\beta_y = \frac{\partial \beta_y}{\partial y}\frac{dy}{dt} + \frac{\partial \beta_y}{\partial x}\frac{dx}{dt}. \tag{6b}$$

Plugging equations (5a) and (5b) into (6a) and (6b) then yields:

$$\frac{d}{dt}\beta_x = \kappa\sigma_{xx}\beta_x\frac{\partial \beta_x}{\partial x} + \kappa\sigma_{yy}\beta_y\frac{\partial \beta_x}{\partial y} \tag{7a}$$

$$\frac{d}{dt}\beta_y = \kappa\sigma_{yy}\beta_y\frac{\partial \beta_y}{\partial y} + \kappa\sigma_{xx}\beta_x\frac{\partial \beta_y}{\partial x}, \tag{7b}$$

which can be written more compactly as:

$$\frac{d\beta}{dt} = \kappa \mathbf{J}\mathbf{M}\beta. \tag{7*}$$

where $\mathbf{J} = \begin{bmatrix} \frac{\partial \beta_x}{\partial x} & \frac{\partial \beta_x}{\partial y} \\ \frac{\partial \beta_y}{\partial x} & \frac{\partial \beta_y}{\partial y} \end{bmatrix}$ is a Jacobian matrix, $\mathbf{M} = \begin{bmatrix} \sigma_{xx} & 0 \\ 0 & \sigma_{yy} \end{bmatrix}$ and $\beta = \begin{bmatrix} \beta_x \\ \beta_y \end{bmatrix}$.

The Jacobian matrix $\mathbf{J}$ plays an important role in the existing theory on multivariate adaptive dynamics, in particular in relation to the convergence stability of an evolutionarily stable strategy (ESS) (i.e., whether nearby resident strategies will converge to the ESS over evolutionary time, see Geritz et al., 1998; McNamara & Leimar, 2020). In general, an ESS is convergence stable if the eigenvalues of the matrix product $\mathbf{JM}$, evaluated at the ESS trait values, have negative real parts. Since the matrix $\mathbf{M}$ is typically unknown, an additional criterion is often useful: Convergence stability is guaranteed for all fixed variance–covariance matrices $\mathbf{M}$ if the matrix $\mathbf{J} + \mathbf{J}^T$ is negative definite at the ESS (McNamara & Leimar, 2020).

Equations (7a) and (7b) describe how changes in the traits x and y affect the selection gradients β_x and β_y, respectively, in the absence of mutational covariance. To understand how changes in each trait feed back to alter the selection gradient β_x acting on the trait x, we can analyse the structure of equation (7a) (see Figure 3B). In fact, there are two feedback components: (1) Direct selection on the focal trait x can affect selection β_x acting on the same trait ("within-trait feedback," $\kappa\sigma_{xx}\beta_x\frac{\partial \beta_x}{\partial x}$: blue arrows in Figure 3B). This is the only type of feedback in the one-trait model presented above (cf. Figure 1). (2) Changes to the other trait y may likewise affect the selection gradient β_x("cross-trait feedback," $\kappa\sigma_{yy}\beta_y\frac{\partial \beta_x}{\partial y}$: green arrows in Figure 3B). Within-trait feedback describes how direct selection on the focal trait affects its selection gradient, whereas cross-trait feedback indicates how interactions between traits influence selection on the focal trait. The structure of feedback on the selection gradient β_y (equation 7b) is analysed analogously in Figure 3(C).

To gain a better understanding of how trait change influences selection, we can analyse the combination of the selection gradient and each feedback component for a given trait (see Figure 2). Similar to the one-trait model, each feedback component can either strengthen or weaken the selection on a focal trait. The overall strength and magnitude of feedback are determined by the sum of the feedback components. We can consequently compare the magnitude of each feedback component to determine which component has a more pronounced effect on the strength of selection acting on the focal trait (see Examples 2 and 3).

The feedback analysis becomes more complicated when mutations have correlated effects on multiple traits (Figure 4). In this case, a trait may change because it is under direct selection, or because it is genetically correlated with other traits that are under selection, as shown in equations (4a) and (4b).

Plugging these equations into (6a) and (6b) then yields:

$$\frac{d}{dt}\beta_x = \kappa\left(\sigma_{xx}\beta_x + \sigma_{xy}\beta_y\right)\frac{\partial \beta_x}{\partial x} + \kappa\left(\sigma_{yy}\beta_y + \sigma_{xy}\beta_x\right)\frac{\partial \beta_x}{\partial y} \tag{8a}$$

$$\frac{d}{dt}\beta_y = \kappa\left(\sigma_{yy}\beta_y + \sigma_{xy}\beta_x\right)\frac{\partial \beta_y}{\partial y} + \kappa\left(\sigma_{xx}\beta_x + \sigma_{xy}\beta_y\right)\frac{\partial \beta_y}{\partial x}. \tag{8b}$$

which can again be written more compactly as equation (7*), this time with a fully general mutational variance–covariance matrix $\mathbf{M} = \begin{bmatrix} \sigma_{xx} & \sigma_{xy} \\ \sigma_{xy} & \sigma_{yy} \end{bmatrix}$.

Equations (8a) and (8b) describe how changes in the traits x and y affect the selection gradients β_x and β_y, respectively, in the presence of mutational covariance. Here, we take equation (8a) as an example to understand how various feedback pathways affect selection on x (Figure 4B). When there is mutational correlation between the two traits, there are four feedback components. Two of these are the same as in the case with no mutational covariance (cf. Figures 3B and 4B): (1) Direct selection on the focal trait x affects selection on the same trait ("within-trait feedback," $\kappa\sigma_{xx}\beta_x\frac{\partial \beta_x}{\partial x}$: blue arrows in Figure 4B). (2) Direct selection on the coevolving trait y affects selection on x ("cross-trait feedback due to direct selection on the coevolving trait," $\kappa\sigma_{yy}\beta_y\frac{\partial \beta_x}{\partial y}$: green arrows in Figure 4B). In addition, there are two feedback components that arise from indirect selection via the mutational correlation between x and y. Such indirect selection may cause either (3) the focal trait x to evolve, leading to "cross-trait feedback due to indirect selection on the focal trait" ($\kappa\sigma_{xy}\beta_y\frac{\partial \beta_x}{\partial x}$: purple arrows in Figure 4B), or (4) the coevolving trait y to evolve, leading to "cross-trait feedback due to indirect selection on the coevolving trait" ($\kappa\sigma_{xy}\beta_x\frac{\partial \beta_x}{\partial y}$: orange arrows in Figure 4B).

Here, the "within-trait feedback"—the first of the four feedback components—describes how direct selection on the focal trait affect its selection gradient (the same as the blue arrows in Figure 3B and C), whereas all the other three feedback components indicate how interactions between the traits influence selection on the focal trait.

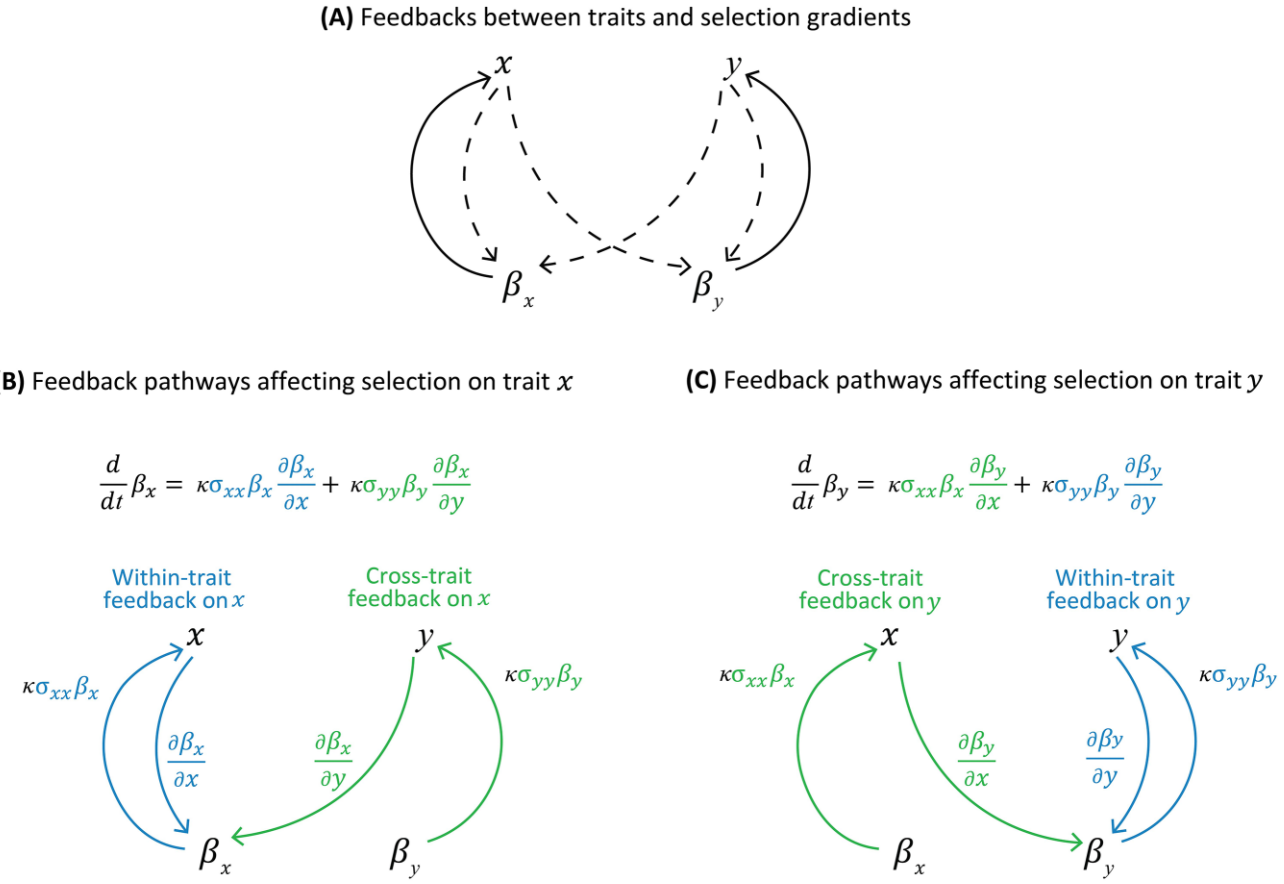

Figure 3. Feedback analysis for two coevolving traits in the absence of mutational covariance. (A) Feedback pathways among the four key elements—the traits x and y and the selection gradients β_x and β_y—when there is no correlation in mutational effects between the two traits. In this case, the selection gradients β_x and β_y influence the respective traits x and y (black solid arrows). Changes in the values of each trait feed back to influence both selection gradients (black dashed arrows). (B) Feedback analysis of the selection gradient β_x in the absence of mutational covariance. Feedback on β_x consists of two components: First, direct selection on the focal trait x feeds back to influence selection β_x on the same trait (blue arrows). This feedback is referred as "within-trait feedback" and quantified as $\kappa\sigma_{xx}\beta_x\frac{\partial\beta_x}{\partial x}$. Only this type of feedback is present in a one-trait model (cf. Figure 1). Second, direct selection on the other trait y affects β_x (green arrows). This feedback is referred as "cross-trait feedback" and quantified as $\kappa\sigma_{yy}\beta_y\frac{\partial\beta_x}{\partial y}$. (C) Feedback analysis of the selection gradient β_y in the absence of mutational covariance. Again, feedback on β_y consists of two components. First, direct selection on the focal trait y feeds back to influence selection β_y on the same trait (blue arrows, "within-trait feedback": quantified as $\kappa\sigma_{yy}\beta_y\frac{\partial\beta_y}{\partial y}$). Second, direct selection on the other trait x affects β_y (green arrows, "cross-trait feedback": quantified as $\kappa\sigma_{xx}\beta_x\frac{\partial\beta_y}{\partial x}$).

Feedback analysis of multivariate evolution

We focused above on the case of two coevolving traits. The extension to multiple traits $(z_1, z_2, \ldots, z_n)$ can be made by setting $\mathbf{J} = \begin{bmatrix} \frac{\partial\beta_1}{\partial z_1} & \frac{\partial\beta_1}{\partial z_2} & \cdots & \frac{\partial\beta_1}{\partial z_n} \\ \frac{\partial\beta_2}{\partial z_1} & \frac{\partial\beta_2}{\partial z_2} & \cdots & \frac{\partial\beta_2}{\partial z_n} \\ \vdots & \vdots & \ddots & \vdots \\ \frac{\partial\beta_n}{\partial z_1} & \frac{\partial\beta_n}{\partial z_2} & \cdots & \frac{\partial\beta_n}{\partial z_n} \end{bmatrix}$, $\mathbf{M} = \begin{bmatrix} \sigma_{11} & \sigma_{12} & \ldots & \sigma_{1n} \\ \sigma_{12} & \sigma_{22} & \ldots & \sigma_{2n} \\ \vdots & \vdots & \ddots & \vdots \\ \sigma_{1n} & \sigma_{2n} & \ldots & \sigma_{nn} \end{bmatrix}$ and $\beta = \begin{bmatrix} \beta_1 \\ \beta_2 \\ \vdots \\ \beta_n \end{bmatrix}$ in equation (7*). Our arguments are thus general and apply also to coevolution among more than two traits. As in the two-trait case, within-trait feedback (e.g., blue arrows in Figures 3 and 4) represents how direct selection on the focal trait affects its selection gradient, whereas all other feedback components describe how interactions between traits influence selection on the focal trait.

Feedback analysis in discrete-time adaptive dynamics

In addition to the continuous-time dynamics outlined above, adaptive dynamics models can also be formulated in discrete time (e.g., Fromhage & Jennions, 2016; Henshaw et al., 2019; Lehtonen & Kokko, 2011). Discrete-time adaptive dynamics can be thought of as an alternative framework in its own right, or as a discrete approximation to the continuous-time dynamics to facilitate the numerical simulation of evolutionary trajectories. In a one-trait model with a resident trait z, the trait value after a discrete time step Δt is approximated by the recursion equation:

$$z_{(t+\Delta t)} \approx z_{(t)} + \frac{1}{2}\mu N\Delta t\sigma_{zz}\beta_z, \tag{9}$$

For simplicity, we write $\delta = \frac{1}{2}\mu N\Delta t$ for the total number of mutations that contribute to evolutionary change over the time step Δt. The discrete-time approximation of the canonical equation can then be written as follows:

$$z_{(t+\Delta t)} \approx z_{(t)} + \delta\sigma_{zz}\beta_z. \tag{9*}$$

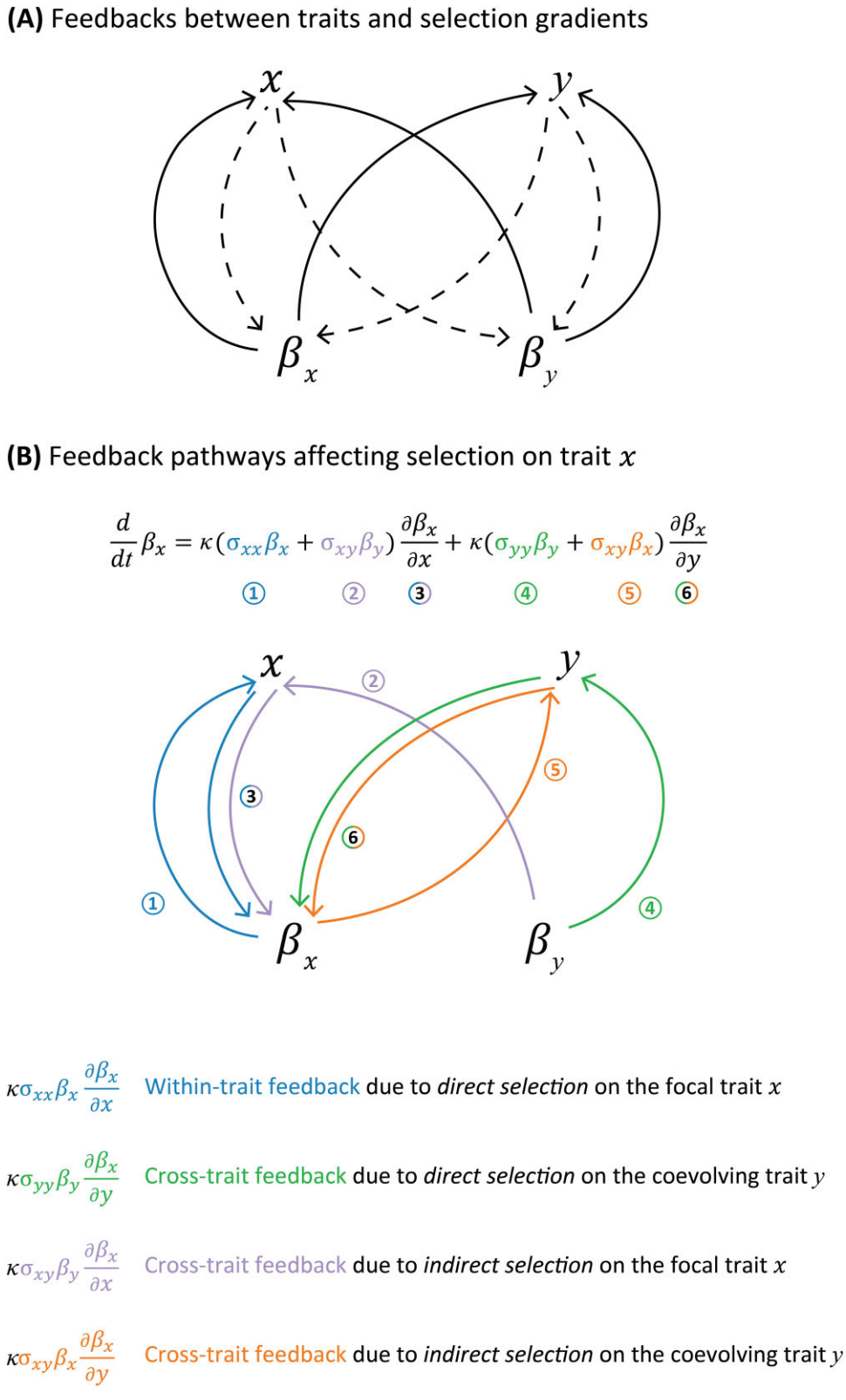

Figure 4. Feedback analysis with mutational covariance between traits. (A) Feedback pathways between trait values and selection gradients in the presence of mutational covariance. In this case, both selection gradients β_x and β_y influence each trait via direct and indirect selection (black solid arrows). Changes in the values of each trait feed back to influence both selection gradients (black dashed arrows). (B) Feedback analysis of the selection gradient β_x in the presence of mutational correlation. Feedback on the selection gradient consists of four components. First, direct selection on the focal trait x feeds back to influence selection β_x on the same trait (blue arrows; quantified as $\kappa\sigma_{xx}\beta_x\frac{\partial\beta_x}{\partial x}$). Second, direct selection on the other trait y affects β_x (green arrows; quantified as $\kappa\sigma_{yy}\beta_y\frac{\partial\beta_x}{\partial y}$). Only these two types of feedback exist in the absence of mutational covariance (cf. Figure 3). Third, indirect selection on the focal trait x due to its correlation with the trait y influences β_x (purple arrows; quantified as $\kappa\sigma_{xy}\beta_y\frac{\partial\beta_x}{\partial x}$). Fourth, indirect selection on the trait y due to its correlation with the focal trait x can also influence β_x (orange arrows; quantified as $\kappa\sigma_{xy}\beta_x\frac{\partial\beta_x}{\partial y}$).

Similarly, in a two-trait model with resident traits x and y, the discrete-time approximation of the canonical equation for each trait is given by:

$$x_{(t+\Delta t)} \approx x_{(t)} + \delta\sigma_{xx}\beta_x + \delta\sigma_{xy}\beta_y \tag{10a}$$

$$y_{(t+\Delta t)} \approx y_{(t)} + \delta\sigma_{yy}\beta_y + \delta\sigma_{xy}\beta_x. \tag{10b}$$

with $\delta = \frac{1}{2}\mu N\Delta t$ defined as above.

The feedback analysis in the discrete-time model is very similar to the continuous-time model shown above. In the discrete-time model, we can approximate the fitness gradients at time $t + \Delta t$ using a first-order Taylor polynomial. For the approximation to be accurate, it is important that the selection gradients are roughly linear as functions of the trait values at the scale of evolutionary change between t and $t + \Delta t$. In other words, changes in mean trait values at this time-scale must be small relative to the radius of curvature of the selection gradients, interpreted as functions of mean trait values. For this to hold, it is sufficient that mutants are similar in phenotype to resident individuals (i.e., the σ_{ij} are small), or that selection gradients are weak (small β_i). These conditions correspond, respectively, to δ-weak and w-weak selection in the sense of Wild & Traulsen (2007). Alternatively, it is sufficient that the time step Δt is small, which might be assumed when the discrete-time adaptive dynamics is used as an approximation to the continuous-time dynamics (e.g., to allow numerical computation of evolutionary trajectories).

Writing the trait values and selection gradients at time $t + \Delta t$ by $(x',\ y')$ and $(\beta_x',\ \beta_y')$, respectively, we have:

$$\beta_x' \approx \beta_x + (x' - x)\frac{\partial}{\partial x}\beta_x + (y' - y)\frac{\partial}{\partial y}\beta_x \tag{11a}$$

$$\beta_y' \approx \beta_y + (x' - x)\frac{\partial}{\partial x}\beta_y + (y' - y)\frac{\partial}{\partial y}\beta_y. \tag{11b}$$

Plugging in equations (10a) and (10b) then yields:

$$\begin{aligned}\beta_x' \approx \beta_x &+ (\delta\sigma_{xx}\beta_x + \delta\sigma_{xy}\beta_y)\frac{\partial}{\partial x}\beta_x \\ &+ (\delta\sigma_{yy}\beta_y + \delta\sigma_{xy}\beta_x)\frac{\partial}{\partial y}\beta_x\end{aligned} \tag{12a}$$

$$\begin{aligned}\beta_y' \approx \beta_y &+ (\delta\sigma_{xx}\beta_x + \delta\sigma_{xy}\beta_y)\frac{\partial}{\partial x}\beta_y \\ &+ (\delta\sigma_{yy}\beta_y + \delta\sigma_{xy}\beta_x)\frac{\partial}{\partial y}\beta_y,\end{aligned} \tag{12b}$$

We can write the equation of (12) more compactly as:

$$\Delta\beta = \beta' - \beta \approx \delta\mathbf{JM}\beta. \tag{12*}$$

with Jacobian matrix $\mathbf{J} = \begin{bmatrix} \frac{\partial\beta_x}{\partial x} & \frac{\partial\beta_x}{\partial y} \\ \frac{\partial\beta_y}{\partial x} & \frac{\partial\beta_y}{\partial y} \end{bmatrix}$, variance–covariance matrix $\mathbf{M} = \begin{bmatrix} \sigma_{xx} & \sigma_{xy} \\ \sigma_{xy} & \sigma_{yy} \end{bmatrix}$, and selection gradients $\beta = \begin{bmatrix} \beta_x \\ \beta_y \end{bmatrix}$. This equation can be analysed analogously to equation (7*) above.

Feedback analysis in the weak selection limit of quantitative genetics

The above approach to selection feedback analysis, based on discrete-time adaptive-dynamic models, can be readily adapted to a class of quantitative-genetic models that assume weak selection. In the weak selection limit, each trait is often assumed to distribute sharply around the mean value (see Iwasa et al., 1991). Under this assumption, the equations for the evolutionary dynamics of quantitative genetic models are analogous in form to the discrete canonical equation of adaptive dynamics (equation 9, cf. Iwasa et al., 1991; Leimar, 2009).

To see how this approach works, we start with a quantitative genetic model of a single trait z. The change in mean trait value $\Delta\bar{z}$ from the current generation to the next generation is given by:

$$\Delta\bar{z} = \mathrm{G}_{zz}\beta_z. \tag{13}$$

where G_{zz} is the additive genetic variance of the trait z, and $\beta_{\bar{z}}$ is the selection gradient, defined in this context as $\beta_z = \frac{1}{\bar{w}}\frac{\partial}{\partial z}(w(z,\bar{z}))|_{z=\bar{z}}$, where $w(z,\bar{z})$ is the fitness of an individual with trait value z in a population with mean trait value $\bar{z}$, and $\bar{w}$ indicates the mean fitness of the population. Note that additive genetic (co)variances in quantitative genetic models often play roles analogous to mutational (co)variances in adaptive dynamics models, although their biological bases differ (see below). In addition, under the weak selection assumption, the definition of the selection gradient coincides with that used in adaptive dynamics (cf. Dieckmann & Law, 1996; Taylor, 1996).

Similarly, the coevolution of two traits, x and y, can be described as

$$\Delta\bar{x} = \mathrm{G}_{xx}\beta_x + \mathrm{G}_{xy}\beta_y \tag{14a}$$

$$\Delta\bar{y} = \mathrm{G}_{yy}\beta_y + \mathrm{G}_{xy}\beta_x, \tag{14b}$$

or more compactly as

$$\begin{bmatrix} \Delta\bar{x} \\ \Delta\bar{y} \end{bmatrix} = \mathbf{G}\beta. \tag{14*}$$

where $\mathbf{G} = \begin{bmatrix} \mathrm{G}_{xx} & \mathrm{G}_{xy} \\ \mathrm{G}_{xy} & \mathrm{G}_{yy} \end{bmatrix}$ is the additive genetic variance–covariance matrix. The **G**-matrix and the **M**-matrix share similar roles in describing variance and covariance in traits. The **M**-matrix describes mutational effects, where the diagonal elements indicate variances in the mutational effects on traits, and the off-diagonal elements are covariances in mutational effects due to pleiotropy (Arnold et al., 2008; Jones et al., 2007). The **G**-matrix, on the other hand, reflects standing genetic variation, with its diagonal consisting of additive genetic variances for traits and its off-diagonal elements capturing additive genetic covariances arising from pleiotropy and linkage disequilibrium (Arnold et al., 2008; Pigliucci, 2006). Despite these similarities, **M**- and **G**-matrices operate on different time scales. The **M**-matrix operates on shorter timescales, highlighting the effects of new mutations as they occur. In contrast, the **G**-matrix is more dynamic and reflects evolutionary processes operating over short, medium, and long-term timescales, incorporating the cumulative effects of mutation, selection, and genetic drift over many generations (Arnold et al., 2008). Both the **G**- and **M**- matrices can evolve over time, yet they are often treated as fixed parameters in mathematical models.

Similar to the discrete-time adaptive dynamics, Taylor series can be used to approximate the fitness gradients (β_x', β_y') at the next time step given the trait value (x', y'), analogously to equations (11 and 12). This gives us:

$$\Delta\beta = \beta' - \beta \approx \mathbf{JG}\beta. \tag{15}$$

with Jacobian matrix $\mathbf{J} = \begin{bmatrix} \frac{\partial \beta_x}{\partial x} & \frac{\partial \beta_x}{\partial y} \\ \frac{\partial \beta_y}{\partial x} & \frac{\partial \beta_y}{\partial y} \end{bmatrix}$, additive genetic variance–covariance matrix $\mathbf{G} = \begin{bmatrix} G_{xx} & G_{xy} \\ G_{xy} & G_{yy} \end{bmatrix}$, and selection gradient $\beta = \begin{bmatrix} \beta_x \\ \beta_y \end{bmatrix}$. Feedback on selection can then be analysed analogously to above.

Examples

To illustrate the application of our feedback analysis, we present three examples. Beginning with an adaptive-dynamic framework, we explore scenarios involving a single trait (Example 1) and two coevolving traits (Example 2). Lastly, we present an example that utilizes the framework of quantitative genetics (Example 3). With these examples, we aim to showcase the versatility and efficacy of our feedback analysis across various evolutionary contexts. Examples 1 and 3 illustrate the application of our approach, serving as practical guides for its implementation. Example 2 highlights both the practical utility and the explanatory power of the framework by applying it to the well-studied evolutionary dynamics underlying the emergence of anisogamy.

Example 1: the evolution of offspring size

We first investigate the evolution of a single trait: offspring size (e.g., the size of eggs at laying or offspring at birth in species with no further parental care), building on the framework established by Smith & Fretwell (1974). The original model was formulated as an optimality model, but we consider it here in an adaptive-dynamic framework. We assume that each female has a fixed amount of resources R for producing offspring. An individual producing offspring of size m can generate $\frac{R}{m}$ offspring in total. Therefore, smaller offspring can be produced in greater number. On the other hand, an offspring's survival probability S increases with its size, which we model following Levitan (2000) as $S = \exp(-\frac{\alpha}{m})$ (see also Bulmer & Parker, 2002; reviewed in Myllymaa & Lehtonen, 2025), where the parameter α scales the relationship between offspring size and survival. There is thus a trade-off between offspring number and survival in this model. The fitness (i.e., the number of surviving offspring) of a rare mutant with offspring size $\hat{m}$ in a resident population with offspring size m is given by $w(\hat{m}, m) = \frac{R}{\hat{m}} \exp(-\frac{\alpha}{\hat{m}})$. Note that selection is frequency-independent in this simple model, so that $w(\hat{m}, m)$ does not depend on the resident strategy m. The selection gradient $\beta_m = \frac{1}{w(m,m)} \frac{\partial}{\partial \hat{m}} w(\hat{m}, m)|_{\hat{m}=m}$, the evolutionary trajectory (obtained from $\frac{dm}{dt} = \kappa \sigma_{mm} \beta_m$) and the feedback acting on the selection gradient ($\frac{d\beta_m}{dt} = \kappa \sigma_{mm} \beta_m \frac{d\beta_m}{dm}$) can be derived easily. Over time, offspring size evolves towards its optimum at $m = \alpha$ (Smith & Fretwell, 1974). The model's simplicity allows for a clear understanding of the dynamics driving selection on offspring size over time.

Figure 5 illustrates an exemplary evolutionary trajectory (Figure 5A), along with the selection gradient (Figure 5B), and the feedback acting on the selection gradient (Figure 5C). Since the initial value of m exceeds the optimal size in this example, it decreases until reaching the optimal size of $m = \alpha = 1$ (Figure 5A). Consequently, the selection gradient is consistently negative (Figure 5B). Feedback is initially negative (to the left of the dashed vertical line in Figure 5C) and then switches to positive (to the right of the dashed vertical line). As offspring size approaches its optimum, both the selection gradient (Figure 5B) and the feedback term (Figure 5C) approach zero. By examining the combination of the selection gradient and its feedback term, we can understand how feedback affects selection (cf. Figure 2). Initially, both the selection gradient and the feedback term are negative. Therefore, as offspring size decreases, selection for smaller size becomes stronger ("negative reinforcing selection," denoted by the blue background in Figure 5C), accelerating the evolutionary process towards the optimal offspring size. This self-reinforcing process continues until around 15 000 units of evolutionary time, at which point the feedback term switches to positive, while the selection gradient remains negative. This reflects "negative inhibiting selection," whereby the selection for smaller offspring weakens as offspring size approaches the equilibrium (purple background in Figure 5C). The transition from self-reinforcing selection to self-inhibiting selection results from the shape of the fitness function. As the trait approaches its equilibrium, where the fitness function is locally concave, the selection gradient decreases in magnitude, indicating inhibiting feedback. However, because the fitness function is not concave across its entire domain, the selection gradient can increase in magnitude over time in certain regions (e.g., at very small or large initial values of offspring size in this case), resulting in stronger directional (reinforcing) selection during the early stages of evolution.

Example 2: the evolution of anisogamy

We next demonstrate the application of our feedback analysis to a model with two coevolving traits: the anisogamy model of Lehtonen & Kokko (2011). In their study, Lehtonen and Kokko (2011) explored the impact of gamete competition and gamete limitation on the evolution of anisogamy. The model considers a population consisting of two different mating types, denoted as x and y, which produce gametes of sizes m_x and m_y, respectively. While both gamete types are initially of similar size, disassortative fusion is necessary to produce zygotes (i.e., type x can only fuse with type y and vice versa). In each local mating group, there are a fixed number of adults, A_x and A_y, of each mating type. Each parent in the group possesses a fixed amount of resources M for reproduction, resulting in the production of a total number of $A_x \frac{M}{m_x}$ and $A_y \frac{M}{m_y}$ gametes with sizes m_x and m_y, respectively. An increase in the values of A_x and A_y corresponds to greater gamete competition. The gametes of each mating type undergo depletion through dying at rates of $\mu(m_x)$ and $\mu(m_y)$, as well as through fertilization occurring at a rate of $\gamma N_x N_y$, where N_x and N_y represent the numbers of gametes with sizes m_x and m_y available for fertilization. Here, the parameter γ determines the encounter rate between the two types of gametes and is used to modify gamete limitation in the model. As illustrated in the Supplementary materials, the dynamics of N_x and N_y are influenced by gamete production, mortality, and fertilization (see equation (S1)). Setting equation (S1) to zero allows the determination of the equilibrium number of available gametes for each mating type.

Similar to the one-trait model shown above, the fitness of each mating type is defined as the total number of surviving zygotes. Therefore, the fitness of a

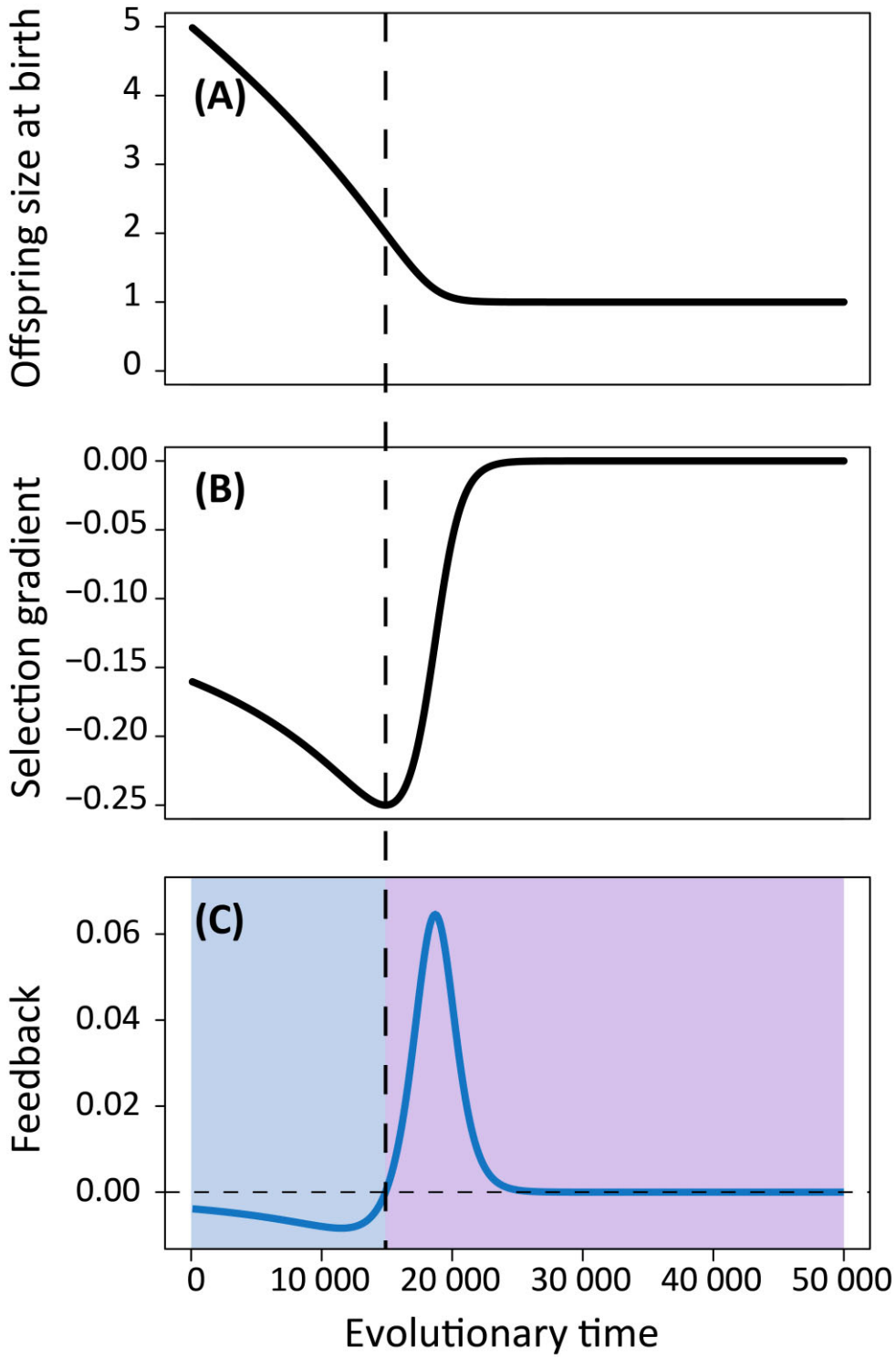

Figure 5. Application of feedback analysis to the evolution of a single trait, offspring size m. (A) Evolutionary trajectory following the canonical equation ($dm/dt = \kappa\sigma_{mm}\beta_m$), (B) selection gradient β_m, and (C) feedback ($d\beta_m/dt = \kappa\sigma_{mm}\beta_m \frac{d\beta_m}{dm}$) over evolutionary time. The vertical dashed line indicates the time point at which the feedback term switches from negative to positive. In (C), the blue and purple backgrounds indicate the "negative reinforcing" and "negative inhibiting" feedback phases, respectively. Parameter settings: $R = 1$, $\alpha = 1$, and $\kappa\sigma_{mm} = 1$. Offspring size m was initialized at 5. We approximated the evolution trajectory, selection gradient, and feedback numerically using Wolfram Mathematica (see Mathematica code available from the Dryad Digital Repository (Long et al. 2025b)).

single mutant which produces gametes of size $\hat{m}_x$ in a resident population with gametes of sizes m_x and m_y is given by $w_x(\hat{m}_x, m_x, m_y) = \gamma \hat{N}_x\, N_y S(\hat{m}_x\, , m_y)$, where $\hat{N}_x$ and N_y are the numbers of gametes with sizes $\hat{m}_x$ and m_y available for fertilization at equilibrium (see equation (S2) in the Supplementary materials) and $S(\hat{m}_x, m_y)$ represents the survival probability of the zygotes, which increases with zygote size (given by $\hat{m}_x + m_y$). The invasion fitness

of a single mutant producing gametes with size $\hat{m}_y$ (i.e., $w_y(\hat{m}_y, m_x, m_y)$) can be derived similarly. Based on the invasion fitness functions, the selection gradients for each gamete type are given by $\beta_{m_x} = \frac{1}{\bar{w}} \frac{\partial}{\partial \hat{m}_x} w_x(\hat{m}_x,\ m_x, m_y)|_{\hat{m}_x = m_x}$ and $\beta_{m_y} = \frac{1}{\bar{w}} \frac{\partial}{\partial \hat{m}_y} w_y(\hat{m}_y,\ m_x, m_y)|_{\hat{m}_y = m_y}$, where $\bar{w}$ indicates the fitness of resident population producing gametes of sizes m_x or m_y (assuming equal sex ratios, we have $\bar{w} = w_x(m_x, m_x, m_y) = w_y(m_y, m_x, m_y)$; see the Supplementary materials for more details).

Lehtonen & Kokko (2011) do not allow for mutational covariance between m_x and m_y. Therefore, both traits are only under direct selection. In line with this, the evolutionary trajectories can be described by our equation (5). Feedback acting on each selection gradient (β_{m_x} and β_{m_y}) due to changes in gamete sizes can be derived using our equation (7).

Figure 6 shows an exemplary evolutionary trajectory, in which an initially small asymmetry in gamete sizes is magnified, ultimately resulting in the evolution of anisogamy. During this process, each selection gradient is shaped by both within- and cross-trait feedback (see Figure 3). Gametes of size m_x are initially slightly smaller than opposite-type gametes, gradually decreasing in size until they reach equilibrium (Figure 6A$_1$). Throughout this process, the selection gradient β_{m_x} remains negative until it stabilizes at zero (Figure 6A$_2$). Within-trait feedback acting on β_{m_x} (i.e., changes in β_{m_x} due to direct selection on m_x) is initially negative (left of the orange dashed vertical line in Figure 6A$_3$), then switches to positive (right of the orange dashed vertical line in Figure 6A$_3$). Given that the selection gradient is uniformly negative (Figure 6A$_2$), this corresponds to an initial phase of reinforcing within-trait feedback, which acts to intensify the negative selection on m_x (blue background in Figure 6A$_3$), followed by inhibiting within-trait feedback that diminishes selection for smaller m_x (purple background in Figure 6A$_3$). This pattern is analogous to feedback on offspring size in the previous example, which starts as a self-reinforcing process but transitions into a self-inhibiting one as the equilibrium is approached. However, this does not fully describe the course of evolution for m_x in this case, as changes in m_y also impact the selection environment for m_x.

Cross-trait feedback on β_{m_x} (i.e., changes in β_{m_x} due to direct selection on m_y) exhibits the opposite pattern to within-trait feedback. It begins as positive (left of the black dashed vertical line in Figure 6A$_4$) and switches to negative (right of the black dashed vertical line in Figure 6A$_4$). The switching point, marked by the black dashed vertical lines in Figure 6, corresponds to a turning point for gametes of size m_y, at which m_y shifts from a decreasing trend to an increasing one (Figure 6B$_1$) and the selection gradient β_{m_y} correspondingly switches from negative to positive (Figure 6B$_2$). Before this switching point, decreasing values of m_y act as a brake on selection for smaller m_x (i.e., negative inhibiting cross-trait feedback; purple background in Figure 6A$_4$), because the need to produce surviving zygotes prevents both gamete types from becoming too small simultaneously. After the switching point, increasing values of m_y accelerate selection for smaller m_x (i.e., negative reinforcing cross-trait feedback; blue background in Figure 6A$_4$). This is because larger values of m_y allow m_x to become even smaller without compromising the viability of zygotes. Within-trait and cross-trait feedback on β_{m_x} act in opposite directions over most of the evolutionary trajectory. By examining the difference between the absolute values of the within- and cross-trait feedback components (indicated by the white dashed lines in Figure 6A$_3$, A$_4$), we can see that inhibiting cross-trait feedback plays a more influential role in the initial evolution of m_x. After m_y begins to increase, there is a brief period in which reinforcing cross-trait feedback dominates, causing selection for smaller m_x to increase. In the final phase, inhibiting within-trait feedback dominates as gamete sizes approach equilibrium.

Gametes of size m_y, which are initially slightly larger than opposite-type gametes, experience an initial decrease in size followed by an increase (Figure 6B$_1$). Correspondingly, the selection gradient β_{m_y} is initially negative, before becoming positive (Figure 6B$_2$). During the period of decreasing m_y (left of the black dashed vertical line in Figure 6B), within-trait feedback follows a pattern very similar to that of m_x. It initially exhibits reinforcing feedback (left of the red dashed vertical line and in blue background in Figure 6B$_3$) and then transitions briefly to inhibiting feedback (between the red and black dashed vertical lines and in purple background in Figure 6B$_3$). Cross-trait feedback is inhibiting throughout initial phase (Figure 6B$_4$). Once m_y starts to increase (right of the black dashed vertical line in Figure 6B), within-trait feedback acts to inhibit selection for larger m_y (purple background in Figure 6B$_3$), whereas cross-trait feedback reinforces this selection (red background in Figure 6B$_4$). As with m_x above, inhibiting cross-trait feedback initially dominates the evolution of the selection gradient. Once m_y begins to increase, reinforcing cross-trait feedback dominates, causing increasing selection for larger m_y. In the final phase, as the equilibrium is approached, inhibiting within-trait feedback exerts a greater influence, leading to a reduction in selection for larger m_y.

Taken together, we gain a comprehensive understanding of the coevolutionary process involving the two gamete types. In the initial phase, both gamete types undergo a decrease in size. This reduction is strongly influenced by cross-trait feedback, which inhibits selection for smaller size in both gamete types, as the costs of reducing gamete size are greater if fertilization partners produce smaller gametes. This aligns with previous arguments that sexual conflict is already present in the earliest stages of the evolution toward anisogamy (Lehtonen et al., 2012). The initially smaller gametes decrease more rapidly, reaching a size that halts further reduction in the opposite type; otherwise, the zygote is unlikely to survive. As the initially smaller gametes continue to decrease in size while the opposite type begins to increase in size, they reinforce the strength of selection on each other via cross-trait feedback, leading to further asymmetry in their sizes. At the end of the coevolutionary process, within-trait feedback becomes more dominant, reducing the strength of selection and causing each type of gamete to evolve slowly toward its equilibrium state.

Example 3: Fisherian runaway process of sexual selection

Our final example, based on the Fisherian runaway process of sexual selection, illustrates the application of feedback analysis in quantitative genetic models. The foundational model for the Fisher process was developed by Lande (1981) (but see Henshaw & Jones, 2020). In this model, populations

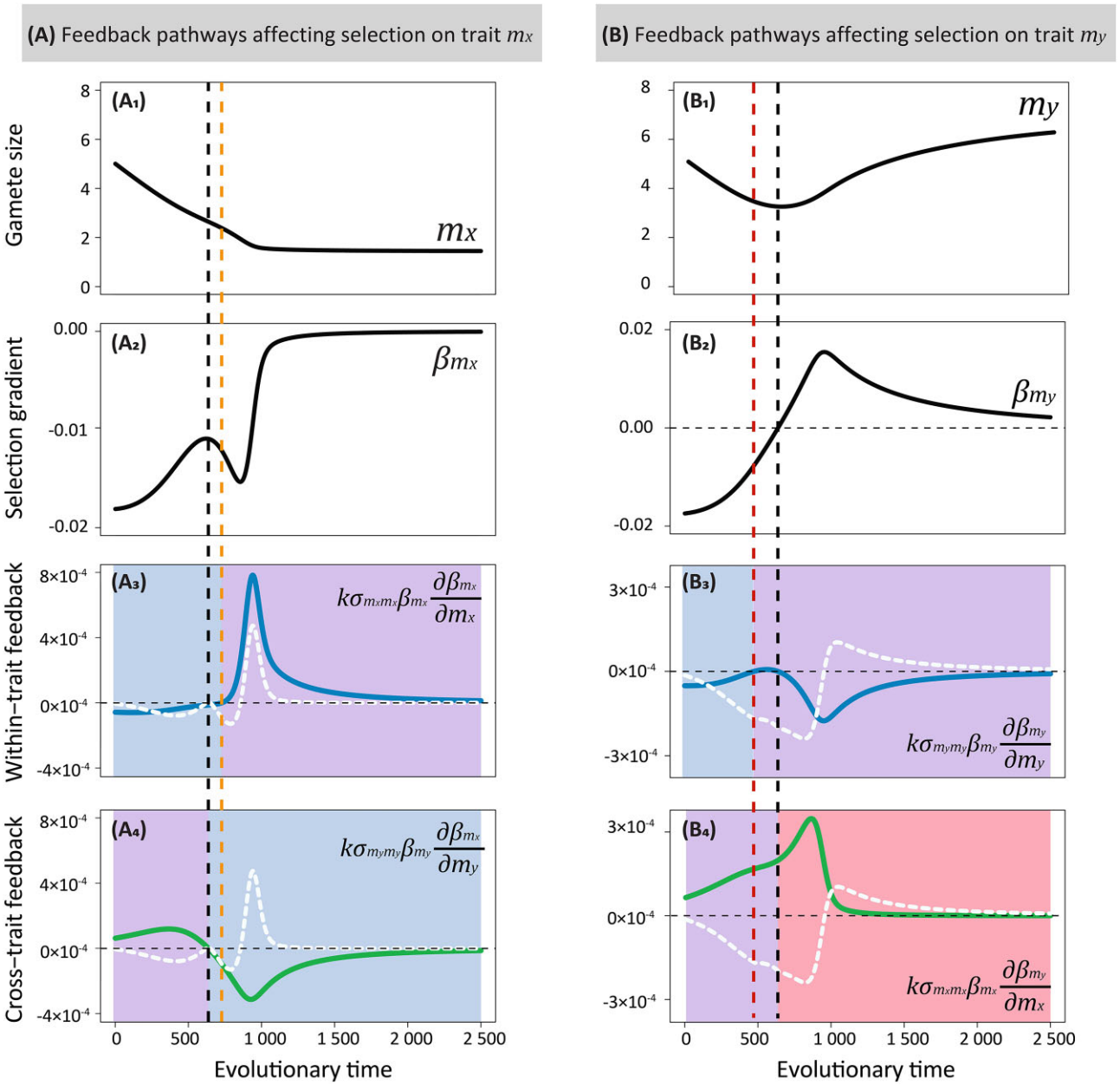

Figure 6. Application of feedback analysis to the evolution of anisogamy. Based on the model of Lehtonen & Kokko (2011), gamete sizes of two mating types, m_x and m_y, coevolve. (A_1, B_1) Evolutionary trajectories of m_x and m_y, following the canonical equation of adaptive dynamics. (A_2, B_2) Selection gradients β_{m_x} and β_{m_y} over evolutionary time. (A_3, B_3) Within-trait feedback (blue lines) on each selection gradient. (A_4, B_4) Cross-trait feedback (green lines) on each selection gradient. The white dashed lines represent the difference in absolute values between within- and cross-trait feedback components, where positive values indicate a greater magnitude of within-trait feedback. The vertical dashed lines (black, orange, and red) indicate the time points at which the feedback components switch sign. The black vertical dashed lines also mark the time point when m_y transitions from a decreasing trend to an increasing one. The blue and red backgrounds indicate "negative reinforcing" and "positive reinforcing" feedback, respectively; and purple background shows all "inhibiting" feedback. Parameter setting: $A_x = A_y = 5$, $M = 1$, $\gamma = 1$, $\kappa = 1$, and $\sigma_{m_x m_x} = \sigma_{m_y m_y} = 1$. Gamete sizes m_x and m_y were initialized at 5 and 5.1, respectively. See detailed model description and other parameter values in the Supplementary materials. We approximated the evolution trajectories, selection gradients, and feedback components numerically using Wolfram Mathematica (see Mathematica code available from the Dryad Digital Repository (Long et al. 2025b)).

are characterized by two quantitative traits: a male ornament s and a female preference p. Both traits are inherited via autosomal transmission and exhibit sex-specific expression. The model assumes no direct benefits or costs for female choosiness and so the selection gradient on female preference is zero. However, indirect selection on preference occurs due to its additive genetic correlation with male ornamentation. Therefore, the changes in the population mean ornament size, $\bar{s}$, and preference, $\bar{p}$, from the current to the next generation can be described as $\Delta\bar{s} = \frac{1}{2}G_{ss}\beta_s$ and $\Delta\bar{p} = \frac{1}{2}G_{sp}\beta_s$, respectively (cf. equation (13)). The factor $\frac{1}{2}$ accounts for sex-specific expression, G_{ss} represents the additive genetic variance for male ornament size, G_{sp} is the additive genetic covariance between male ornament size and female preference strength, and β_s is the selection gradient for the male ornament. In the model of Lande (1981), the fitness of a male

with ornament size s in a population with mean preference $\bar{p}$ is given by $w(s, \bar{p}) = v(s)\varphi(s, \bar{p})$. Here, the viability function $v(s) = \exp[-\frac{1}{2}\frac{(s-\theta)^2}{\omega^2}]$ determines the survival probability of a male with ornament size s (where $1/\omega$ reflects the strength of viability selection against exaggerated ornaments and θ is the optimal ornament size under viability selection). The "psychophysical" preference function $\varphi(s, \bar{p}) = \exp(s\bar{p})$ determines the mating success of a male with ornament size s in a population with the mean female preference strength $\bar{p}$. Females with $p > 0$ prefer males with more extreme ornamentation. The selection gradient for the male ornament is therefore given by $\beta_s = \frac{1}{w(\bar{s}, \bar{p})}\frac{\partial}{\partial s}(w(s, \bar{p}))|_{s=\bar{s}} = \bar{p} - \frac{\bar{s}-\theta}{\omega^2}$. Setting the selection gradient equal to zero yields a line of equilibria for female preference and male ornament: $\bar{p} = \frac{\bar{s}-\theta}{\omega^2}$, with the slope given by $\frac{1}{\omega^2}$.

By applying equation (15) , we can analyse how changes in male ornamentation and female preference influence selection on $\bar{s}$. Since the selection gradient β_s is a linear function of trait values in Lande's model, the assumption of weak selection is not strictly required here, although in most other cases it will be. There are two feedback components at play here: within-trait feedback (given by $\delta G_{ss}\beta_s\frac{\partial}{\partial \bar{s}}\beta_s = -\frac{1}{\omega^2}\delta G_{ss}\beta_s$), and cross-trait feedback due to indirect selection on female preference (given by $\delta G_{sp}\beta_s\frac{\partial}{\partial \bar{p}}\beta_s = \delta G_{sp}\beta_s$). For a better understanding, we here focus on the case where the male ornament is initialized with a value smaller than the optimal size ($s < \theta$), and thus, there is selection favoring larger male ornament ($\beta_s > 0$). Accordingly, the within-trait feedback $-\frac{1}{\omega^2}\delta G_{ss}\beta_s$ becomes negative, suggesting that as male ornament size increases, selection for further enlargement diminishes. This self-inhibiting phenomenon arises due to male ornamentation approaching its optimal size for a fixed preference strength. On the other hand, the cross-trait feedback $\delta G_{sp}\beta_s$ is positive, indicating a positive reinforcing effect. This means that as female preference increases, selection for even larger male ornaments is enhanced.

By comparing the magnitudes of each feedback component ($|-\frac{1}{\omega^2}\delta G_{ss}\beta_s|$ vs. $|\delta G_{sp}\beta_s|$), we can understand how they interact with the selection gradient (note that we focus on the case of $\beta_s > 0$), thereby influencing the evolution of male ornamentation and female preference. When the within-trait feedback is larger in magnitude ($G_{sp}/G_{ss} < \frac{1}{\omega^2}$), selection for larger male ornamentation is predominantly inhibiting until it reaches the equilibrium. This inhibiting effect extends to the genetically correlated female preference, resulting in a similar evolutionary trajectory. Therefore, in this case the evolution will proceed towards the line of equilibria with slope $\frac{1}{\omega^2}$. In contrast, when the cross-trait feedback has is larger in magnitude ($G_{sp}/G_{ss} > \frac{1}{\omega^2}$), increases in female preference further amplify selection for even larger ornament in males, resulting in a never-ending runaway process. This process accelerates rapidly away from any equilibrium point, with traits evolving at an ever-increasing speed. Our framework therefore provides a new lens through which to view Lande's (1981) original analysis.

Discussion

In this study, we provide a general framework for quantifying how changes in coevolving traits, caused by selection, feed back to shape the selection environment. This framework can be applied both to adaptive-dynamic models and to quantitative-genetic models that assume weak selection. Our framework can be used to provide formal support or refutation of verbal arguments about exactly why certain traits coevolve in the manner they do.

The application of our framework to the evolution of anisogamy (Example 2) illustrates its power for interrogating verbal models of coevolution. In the model we analyse, small initial asymmetries in gamete size can amplify over evolutionary time, leading to divergence into small gametes (sperm) and large gametes (eggs). Trivers (1972) famously argued that any initial differences in parental investment between the sexes are maintained or magnified over time a via self-reinforcing process. Trivers' argument was as follows: Because females initially invest more than males in zygotes, they have more to lose if they abandon their offspring and so should be incentivized to provide further parental investment (e.g., larger eggs or postzygotic care). In contrast, males, who invest less in gametes and consequently become mate-limited, should allocate more resources to competitive traits to enhance their mating success, rather than increasing parental investment. This argument has been criticized for various reasons (e.g., it commits the "Concorde fallacy"; see Dawkins & Carlisle, 1976; Kokko & Jennions, 2008). Some authors argue that anisogamy may not be the fundamental cause of sex-role divergence (Ah-King, 2013; Gowaty & Hubbell, 2005), while others have suggested that anisogamy can drive sex-role divergence when other factors are taken into account (e.g., Fromhage & Jennions, 2016; Lehtonen et al., 2016; Queller, 1997; Schärer et al., 2012).

Our feedback analysis of the evolution of anisogamy suggests a new take on Trivers' argument: In our analysis, sex differences in gamete investment are not maintained by a self-reinforcing process ('I should invest more because I already invested more'), but rather by a cross-trait reinforcing process ('I should invest more because my partner invested less' and 'I should invest less because my partner invested more'). Importantly, reinforcement here occurs over evolutionary time, rather than within a generation. As depicted in Figure 6, if one gamete type is larger than the other, the selection environment for each gamete type is strongly shaped by cross-trait reinforcing feedback. The decreasing size of the smaller gamete creates a selection environment that favors even larger size in the larger gamete. Similarly, the increasing size of the larger gamete selects for further reductions in the size of the smaller gamete. In contrast to Trivers' argument, changes in the size of one gamete type often lead to *weaker* selection for further changes in the same direction (within-trait inhibiting feedback). An analogous argument could potentially be developed to explain the divergence of postzygotic parental investment (cf. McNamara et al., 2003), the main target of Trivers' original argument, although careful consideration would be needed to account for the differences in the selection pressures acting on gamete size and subsequent parental investment.

To apply our framework in a discrete-time setting, a key assumption must be satisfied: The selection gradients must be nearly linear over the scale of microevolutionary change. This restriction is required because we approximate the selection gradients using a first-order Taylor polynomial (i.e., a linear approximation) when estimating how they change due to trait evolution. Typically, this assumption is framed as "weak selection," since it is met when evolution is

gradual (McElreath & Boyd, 2008; Wild & Traulsen, 2007). In adaptive dynamics, weak selection is typically assumed as part of the framework's foundation, whereas in quantitative genetic models, it is an additional assumption. Under strong selection, our feedback framework should be viewed only as an approximation. This is because, in such cases, the feedback components (i.e., within- and cross-trait feedback as demonstrated in our study) do not interact additively, posing challenges in disentangling the contribution of each feedback component to changes in selection environment. Given the key assumptions of our framework, our feedback analysis could feasibly be extended to population genetic models, particularly in scenarios involving weak selection (Barton & Turelli, 1991; Kirkpatrick et al., 2002; van Doorn & Kirkpatrick, 2010). However, the genetic details, including factors such as dominance and epistasis, along with interactions between multiple genetic loci, can lead to more complex coevolutionary dynamics. Therefore, it may be necessary to account for these factors when extending the framework.

Our framework assumes that mean trait values alone are sufficient to determine evolutionary dynamics. This simplification is insufficient to capture some important evolutionary phenomena, however. For example, in some adaptive-dynamic models, the dynamics lead to evolutionary branching (Geritz et al., 1998). Branching corresponds to an increase in phenotypic variance that results in polymorphic populations with a bimodal distribution of traits (Dercole & Rinaldi, 2008; Geritz et al., 1998). Our approach as developed here cannot provide insights once traits converge to a branching point. Further, both the **M**-matrix and the **G**-matrix may evolve, rather than being fixed as we assume here (Arnold et al., 2008; Blows, 2007; Jones et al., 2007). This in turn may feed back to influence the strength and direction of selection. While the framework developed here assumes that selection is sensitive to trait means only, future work could extend this framework to consider how changes in trait distributions more broadly shape the selection environment.

While our framework is grounded in evolutionary theory via adaptive dynamics and quantitative genetics, its structure also shares similarities with recent advances in analysing feedbacks in ecoevolutionary dynamics (e.g., Hairston et al., 2005; Patel et al., 2018). A common feature of both is the focus on partitioning the contributions of specific feedback pathways, thereby identifying and interpreting the mechanisms that drive dynamics over time. This perspective aligns closely with the core principles of system dynamics (Forrester, 1982, 1983), particularly when combined with feedback loop analysis methods (Kampmann, 2012; Kampmann & Oliva, 2006, 2008), which use the system's Jacobian matrix as the basis for identifying feedback loops and linking them to the system's stability properties. Similar to (eco-)evolutionary feedback analysis, these methods track how changes in system behavior are driven by shifts in individual feedback loops over time. Reinforcing loops tend to generate accelerating increases or decreases and, when sufficiently strong relative to balancing loops, can promote instability. Conversely, balancing loops counteract change and thereby promote stability. Such methods have been applied widely across complex systems, including ecology (e.g., Abram & Dyke, 2018) and social–ecological research (e.g., Lade et al., 2015). Situating our work within this broader tradition underscores its generality and relevance to the study of complex adaptive systems.

Supplementary material

Supplementary material is available online at *Evolution*.

Data availability

The Mathematica scripts used for performing the feedback analysis in Examples 1 and 2 of this study, along with the generated data, are available for download from Dryad Digital Repository (https://doi.org/10.5061/dryad.8w9ghx419; Long et al., 2025b).

Author contributions

X.L. and J.M.H. came up with the original idea; X.L. and J.M.H. developed the methods; all three authors contributed by discussing theory, methods and concepts. X.L. wrote the manuscript; all three authors revised the manuscript.

Funding

X.L. and J.M.H. were funded by the Bundesministerium fu¨r Bildung und Forschung, Germany, and the Deutsche Forschungsgemeinschaft (DFG, German Research Foundation) under project number 456626331. J.L. was funded by an Academy of Finland grant (340130).

Conflict of interest

No competing interest is declared. Editorial processing of the manuscript was conducted independently of J.M.H., who is an Associate Editor of *Evolution*.

Acknowledgments

We thank Geoff Parker for helpful discussions related to the work. We are grateful to the two anonymous reviewers and the editors for their thoughtful and valuable comments.

References

Abram, J. J., & Dyke, J. G. (2018). Structural loop analysis of complex ecological systems. *Ecological Economics*, *154*, 333–342. https://doi.org/10.1016/j.ecolecon.2018.08.011

Ah-King, M. (2013). On anisogamy and the evolution of 'sex roles'. *Trends in Ecology & Evolution*, *28*(1), 1–2. https://doi.org/10.1016/j.tree.2012.04.004

Andersson, M. (1994). *Sexual selection*. Princeton University Press. https://doi.org/10.1515/9780691207278

Arnold, S. J., Bürger, R., Hohenlohe, P. A., Ajie, B. C., & Jones, A. G. (2008). Understanding the evolution and stability of the G-matrix. *Evolution*, *62*(10), 2451–2461. https://doi.org/10.1111/j.1558-5646.2008.00472.x

Baldauf, S. A., Engqvist, L., & Weissing, F. J. (2014). Diversifying evolution of competitiveness. *Nature Communications*, *5*(1), 5233. https://doi.org/10.1038/ncomms6233

Bank, C. (2022). Epistasis and adaptation on fitness landscapes. *Annual Review of Ecology, Evolution, and Systematics*, *53*(1), 457–479. https://doi.org/10.1146/annurev-ecolsys-102320-112153

Barton, N. H., & Turelli, M. (1991). Natural and sexual selection on many loci. *Genetics*, *127*(1), 229–255. https://doi.org/10.1093/genetics/127.1.229

Blows, M. W. (2007). A tale of two matrices: multivariate approaches in evolutionary biology. *Journal of Evolutionary Biology*, *20*(1), 1–8. https://doi.org/10.1111/j.1420-9101.2006.01164.x

Bulmer, M. G., & Parker, G. A. (2002). The evolution of anisogamy: a game-theoretic approach. *Proceedings of the Royal Society of London. Series B: Biological Sciences*, *269*(1507), 2381–2388. https://doi.org/10.1098/rspb.2002.2161

Champagnat, N., Ferriere, R., & Ben Arous, G. (2001). The canonical equation of adaptive dynamics: a mathematical view. *Selection*, *2*, 71–81.

Dashtbali, M., Long, X., & Henshaw, J. M. (2024). The evolution of honest and dishonest signals of fighting ability. *Evolution Letters*, *8*, qrae008.

Dawkins, R., & Carlisle, T. R. (1976). Parental investment, mate desertion and a fallacy. *Nature*, *262*(5564), 131–133. https://doi.org/10.1038/262131a0

Dercole, F., & Rinaldi, S. (2008). *Analysis of evolutionary processes: The adaptive dynamics approach and its applications: The adaptive dynamics approach and its applications*. Princeton University Press. https://doi.org/10.1515/9781400828340

Dieckmann, U., & Law, R. (1996). The dynamical theory of coevolution: A derivation from stochastic ecological processes. *Journal of Mathematical Biology*, *34*, 579–612. https://doi.org/10.1007/BF02409751

Fawcett, T. W., Kuijper, B., Weissing, F. J., & Pen, I. (2011). Sex-ratio control erodes sexual selection, revealing evolutionary feedback from adaptive plasticity. *Proceedings of the National Academy of Sciences*, *108*(38), 15925–15930. https://doi.org/10.1073/pnas.1105721108

Forrester, N. B. (1982). *A dynamic synthesis of basic macroeconomic theory: Implications for stabilization policy analysis*. [PhD Thesis. Sloan School of Management].

Forrester, N. (1983). Eigenvalue analysis of dominant feedback loops. In *Plenary session papers proceedings of the 1st international system dynamics society conference*. (pp. 178–202). System Dynamics Society.

Fromhage, L., & Jennions, M. D. (2016). Coevolution of parental investment and sexually selected traits drives sex-role divergence. *Nature Communications*, *7*(1), 12517. https://doi.org/10.1038/ncomms12517

Geritz, S. A., Kisdi, E., Meszé NA, G., & Metz, J. A. (1998). Evolutionarily singular strategies and the adaptive growth and branching of the evolutionary tree. *Evolutionary Ecology*, *12*, 35–57. https://doi.org/10.1023/A:1006554906681

Giraldeau, L. A., & Caraco, T. (2000). *Social foraging theory*. (Vol. *73*). Princeton University Press. https://doi.org/10.1515/9780691188348

Gowaty, P. A. (2005). Chance, time allocation, and the evolution of adaptively flexible sex role behavior. *Integrative and Comparative Biology*, *45*(5), 931–944. https://doi.org/10.1093/icb/45.5.931

Hairston, N. G., Ellner, S. P., Geber, M. A., Yoshida, T., & Fox, J. A. (2005). Rapid evolution and the convergence of ecological and evolutionary time. *Ecology Letters*, *8*(10), 1114–1127. https://doi.org/10.1111/j.1461-0248.2005.00812.x

Harten, L., Matalon, Y., Galli, N., Navon, H., Dor, R., & Yovel, Y. (2018). Persistent producer-scrounger relationships in bats. *Science Advances*, *4*(2), e1603293. https://doi.org/10.1126/sciadv.1603293

Henshaw, J. M., Fromhage, L., & Jones, A. G. (2019). Sex roles and the evolution of parental care specialization. *Proceedings of the Royal Society B: Biological Sciences*, *286*(1909), 20191312. https://doi.org/10.1098/rspb.2019.1312

Henshaw, J. M., & Jones, A. G. (2020). Fisher's lost model of runaway sexual selection. *Evolution*, *74*(2), 487–494. https://doi.org/10.1111/evo.13910

Hochberg, M. E., Rankin, D. J., & Taborsky, M. (2008). The coevolution of cooperation and dispersal in social groups and its implications for the emergence of multicellularity. *BMC Evolutionary Biology*, *8*, 1–14. https://doi.org/10.1186/1471-2148-8-238

Iwasa, Y., Pomiankowski, A., & Nee, S. (1991). The evolution of costly mate preferences II. The "handicap" principle. *Evolution*, *45*(6), 1431–1442.

Jones, A. G., Arnold, S. J., & Bürger, R. (2007). The mutation matrix and the evolution of evolvability. *Evolution*, *61*(4), 727–745. https://doi.org/10.1111/j.1558-5646.2007.00071.x

Kampmann, C. E., & Oliva, R. (2006). Loop eigenvalue elasticity analysis: Three case studies. *System Dynamics Review*, *22*(2), 141–162. https://doi.org/10.1002/sdr.333

Kampmann, C. E., & Oliva, R. (2008). Structural dominance analysis and theory building in system dynamics. *Systems Research and Behavioral Science*, *25*(4), 505–519. https://doi.org/10.1002/sres.909

Kampmann, C. E. (2012). Feedback loop gains and system behavior (1996). *System Dynamics Review*, *28*(4), 370–395. https://doi.org/10.1002/sdr.1483

Kirkpatrick, M. (1982). Sexual selection and the evolution of female choice. *Evolution*, *36*, 1–12. https://doi.org/10.2307/2407961

Kirkpatrick, M., Johnson, T., & Barton, N. (2002). General models of multilocus evolution. *Genetics*, *161*(4), 1727–1750. https://doi.org/10.1093/genetics/161.4.1727

Kokko, H., & Jennions, M. D. (2008). Parental investment, sexual selection and sex ratios. *Journal of Evolutionary Biology*, *21*(4), 919–948. https://doi.org/10.1111/j.1420-9101.2008.01540.x

Kuijper, B., Pen, I., & Weissing, F. J. (2012). A guide to sexual selection theory. *Annual Review of Ecology, Evolution, and Systematics*, *43*(1), 287–311. https://doi.org/10.1146/annurev-ecolsys-110411-160245

Lade, S. J., Niiranen, S., Hentati-Sundberg, J., Blenckner, T., Boonstra, W. J., Orach, K., Quaas, M. F., Österblom, H., & Schlüter, M. (2015). An empirical model of the Baltic Sea reveals the importance of social dynamics for ecological regime shifts. *Proceedings of the National Academy of Sciences*, *112*(35), 11120–11125. https://doi.org/10.1073/pnas.1504954112

Lande, R. (1981). Models of speciation by sexual selection on polygenic traits. *Proceedings of the National Academy of Sciences*, *78*(6), 3721–3725. https://doi.org/10.1073/pnas.78.6.3721

Lande, R., & Arnold, S. J. (1983). The measurement of selection on correlated characters. *Evolution*, *37*, 1210–1226. https://doi.org/10.2307/2408842

Lehtonen, J., & Kokko, H. (2011). Two roads to two sexes: unifying gamete competition and gamete limitation in a single model of anisogamy evolution. *Behavioral Ecology and Sociobiology*, *65*, 445–459. https://doi.org/10.1007/s00265-010-1116-8

Lehtonen, J., Jennions, M. D., & Kokko, H. (2012). The many costs of sex. *Trends in Ecology & Evolution*, *27*(3), 172–178. https://doi.org/10.1016/j.tree.2011.09.016

Lehtonen, J., Parker, G. A., & Schärer, L. (2016). Why anisogamy drives ancestral sex roles. *Evolution*, *70*(5), 1129–1135. https://doi.org/10.1111/evo.12926

Leimar, O. (2009). Multidimensional convergence stability. *Evolutionary Ecology Research*, *11*(2), 191–208.

Levitan, D. R. (2000). Optimal egg size in marine invertebrates: Theory and phylogenetic analysis of the critical relationship between egg size and development time in echinoids. *The American Naturalist*, *156*(2), 175–192. https://doi.org/10.1086/303376

Long, X., & Weissing, F. J. (2023). Transient polymorphisms in parental care strategies drive divergence of sex roles. *Nature Communications*, *14*(1), 6805. https://doi.org/10.1038/s41467-023-42607-6

Long, X., Székely, T., Komdeur, J., & Weissing, F. J. (2025a). A life history perspective on the evolutionary interplay of sex ratios and parental sex roles. *The American Naturalist*, *205*(2), E49–E65. https://doi.org/10.1086/733457

Long, X., Lehtonen, J., & Henshaw, M. J. (2025b). Mathematica scripts and related data from: quantifying feedback among traits in coevolutionary models. *Dryad*. https://doi.org/10.5061/dryad.8w9ghx419

Maisonneuve, L., & Aubier, T. G. (2025). The "sexual selection hypothesis" for the origin of aposematism. *Evolution*, *79*, qpaf030.

Mathot, K. J., & Giraldeau, L. A. (2008). Increasing vulnerability to predation increases preference for the scrounger foraging tactic. *Behavioral Ecology*, *19*(1), 131–138. https://doi.org/10.1093/beheco/arm114

McElreath, R., & Boyd, R. (2008). *Mathematical models of social evolution: A guide for the perplexed*. University of Chicago Press.

McGill, B. J., & Brown, J. S. (2007). Evolutionary game theory and adaptive dynamics of continuous traits. *Annual Review of Ecology, Evolution, and Systematics*, *38*(1), 403–435. https://doi.org/10.1146/annurev.ecolsys.36.091704.175517

McNamara, J. M., & Leimar, O. (2020). *Game theory in biology: Concepts and frontiers*. Chapter 6. Oxford University Press. https://doi.org/10.1093/oso/9780198815778.001.0001

McNamara, J. M. (2003). Should young ever be better off with one parent than with two?. *Behavioral Ecology*, *14*(3), 301–310. https://doi.org/10.1093/beheco/14.3.301

Mead, L. S., & Arnold, S. J. (2004). Quantitative genetic models of sexual selection. *Trends in Ecology & Evolution*, *19*(5), 264–271. https://doi.org/10.1016/j.tree.2004.03.003

Mullon, C., Keller, L., & Lehmann, L. (2018). Social polymorphism is favoured by the co-evolution of dispersal with social behaviour. *Nature Ecology & Evolution*, *2*(1), 132–140. https://doi.org/10.1038/s41559-017-0397-y

Myllymaa, L., & Lehtonen, J. (2025). Zygote survival functions: A critical systematisation. *Methods in Ecology and Evolution*, *00*, 1–13.

Nagylaki, T. (1992). *Introduction to theoretical population genetics*. (Vol.*21*). Springer Science & Business Media.

Patel, S., Cortez, M. H., & Schreiber, S. J. (2018). Partitioning the effects of eco-evolutionary feedbacks on community stability. *The American Naturalist*, *191*(3), 381–394. https://doi.org/10.1086/695834

Pen, I., & Weissing, F. J. (2001). Sexual selection and the sex ratio: An ESS analysis. *Selection*, *1*(1-3), 111–122. https://doi.org/10.1556/Select.1.2000.1-3.11

Pigliucci, M. (2006). Genetic variance–covariance matrices: A critique of the evolutionary quantitative genetics research program. *Biology & Philosophy*, *21*, 1–23. https://doi.org/10.1007/s10539-005-0399-z

Powers, S. T., Penn, A. S., & Watson, R. A. (2011). The concurrent evolution of cooperation and the population structures that support it. *Evolution*, *65*(6), 1527–1543. https://doi.org/10.1111/j.1558-5646.2011.01250.x

Queller, D. C. (1997). Why do females care more than males? *Proceedings of the Royal Society of London. Series B: Biological Sciences*, *264*(1388), 1555–1557. https://doi.org/10.1098/rspb.1997.0216

Ranta, E. S. A., Peuhkuri, N., Hirvonen, H., & Barnard, C. J. (1998). Producers, scroungers and the price of a free meal. *Animal Behaviour*, *55*(3), 737–744. https://doi.org/10.1006/anbe.1997.0649

Revathi Venkateswaran, V., Roth, O., & Gokhale, C. S. (2021). Consequences of combining sex-specific traits. *Evolution*, *75*(6), 1274–1287. https://doi.org/10.1111/evo.14204

Roff, D. A. (1997). *Evolutionary quantitative genetics*. Springer Science & Business Media. https://doi.org/10.1007/978-1-4615-4080-9

Schärer, L., Rowe, L., & Arnqvist, G. (2012). Anisogamy, chance and the evolution of sex roles. *Trends in Ecology & Evolution*, *27*(5), 260–264. https://doi.org/10.1016/j.tree.2011.12.006

Smith, C. C., & Fretwell, S. D. (1974). The optimal balance between size and number of offspring. *The American Naturalist*, *108*(962), 499–506. https://doi.org/10.1086/282929

Svensson, E. I., Arnold, S. J., Bürger, R., Csilléry, K., Draghi, J., Henshaw, J. M., Jones, A. G., De Lisle, S., Marques, D. A., McGuigan, K., Simon, M. N., & Runemark, A. (2021). Correlational selection in the age of genomics. *Nature Ecology & Evolution*, *5*(5), 562–573. https://doi.org/10.1038/s41559-021-01413-3

Taylor, P. D. (1996). The selection differential in quantitative genetics and ESS models. *Evolution*, *50*, 2106–2110. https://doi.org/10.2307/2410769

Trivers, R. L. (1972). Parental investment and sexual selection. In L. D. Houck, & L. C. Drickamer (Eds.), *Sexual selection and the descent of man 1871–1971*. University of Chicago Press.

van Doorn, G. S., & Kirkpatrick, M. (2010). Transitions between male and female heterogamety caused by sex-antagonistic selection. *Genetics*, *186*(2), 629–645. https://doi.org/10.1534/genetics.110.118596

Waffender, A., & Henshaw, J. M. (2023). Long-term persistence of exaggerated ornaments under Fisherian runaway despite costly mate search. *Journal of Evolutionary Biology*, *36*(1), 45–56. https://doi.org/10.1111/jeb.14127

Wild, G., & Traulsen, A. (2007). The different limits of weak selection and the evolutionary dynamics of finite populations. *Journal of Theoretical Biology*, *247*(2), 382–390. https://doi.org/10.1016/j.jtbi.2007.03.015

Received May 9, 2025; revisions received September 3, 2025; accepted September 14, 2025
Associate Editor: Vincent Calcagno; Handling Editor: Jason Wolf